

# RADA: Robust and Accurate Feature Learning with Domain Adaptation

Jingtai He, Gehao Zhang, Tingting Liu, and Songlin Du

School of Automation, Southeast University, Nanjing 210096, China  
{hejingtai,sdu}@seu.edu.cn

**Abstract.** Recent advancements in keypoint detection and descriptor extraction have shown impressive performance in local feature learning tasks. However, existing methods generally exhibit suboptimal performance under extreme conditions such as significant appearance changes and domain shifts. In this study, we introduce a multi-level feature aggregation network that incorporates two pivotal components to facilitate the learning of robust and accurate features with domain adaptation. First, we employ domain adaptation supervision to align high-level feature distributions across different domains to achieve invariant domain representations. Second, we propose a Transformer-based booster that enhances descriptor robustness by integrating visual and geometric information through wave position encoding concepts, effectively handling complex conditions. To ensure the accuracy and robustness of features, we adopt a hierarchical architecture to capture comprehensive information and apply meticulous targeted supervision to keypoint detection, descriptor extraction, and their coupled processing. Extensive experiments demonstrate that our method, RADA, achieves excellent results in image matching, camera pose estimation, and visual localization tasks.

**Keywords:** Local features · Domain adaptation · Descriptor enhancement · Image matching

## 1 Introduction

Robust and accurate keypoint detection and descriptor extraction are fundamental for various computer vision tasks, such as visual localization [23], and structure from motion (SfM) [11]. With the advent of deep learning, significant advancements [5,6,14] have been achieved, enhancing both the accuracy and efficiency of local features compared to traditional handcrafted methods [10,17].

The adoption of sparse-to-sparse feature learning, which follows a 'detect-then-describe' paradigm, has proven common and effective in feature matching methodologies [31]. Numerous methods adhering to this paradigm have been developed, focusing on optimizing individual components, such as keypoint detection or descriptor extraction, to enhance the local features. Nevertheless, the robustness of these features can significantly deteriorate under extreme domain variations, such as day-night changes or different seasons. This deterioration

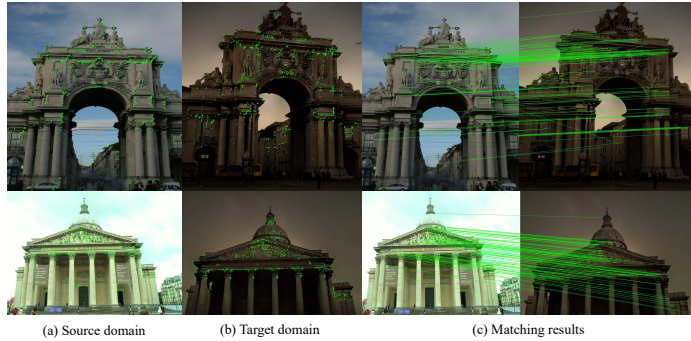


Fig. 1: The visualization of detected keypoints and the matches using our RADA on the Megadepth [9] validation set. (a) Keypoints detection from the source domain (daytime). (b) Keypoints detection from the target domain (nighttime). (c) The matching results of image pairs composed of different source and target domain images. The green lines show correct correspondences.

occurs because the keypoint detection stage is susceptible to variations in low-level image statistics, which affects the subsequent feature descriptors’ ability to maintain invariance. To mitigate this challenge, we draw inspiration from transfer learning [7] and propose domain adaptation supervision implemented prior to the keypoint detection stage. This component aims to establish a mapping between different domains, thereby minimizing discrepancies in high-level feature distributions. By aligning these distributions, we improve keypoint detector stability, the robustness and invariance of descriptors across varying conditions.

Under large illumination and viewpoint changes, local visual information becomes unreliable and indistinguishable, leading to the degradation of descriptors. To address this issue, the global modeling capability of Transformer has been increasingly utilized to incorporate contextual information into feature descriptors, enhancing their robustness [13,27,28]. Motivated by these advancements, we develop a Transformer-based booster designed to boost the robustness and accuracy of descriptors by integrating both the visual and geometric information from all keypoints into individual descriptors. A noteworthy aspect of our approach is the use of a wave-based position encoder, which offers enhanced encoding capabilities. Leveraging the global receptive field in Transformer, the boosted descriptors encapsulate global contextual information, thereby becoming more robust and discriminative.

In summary, the main contributions of this paper are as follows:

- We introduce domain adaptation supervision to align high-level feature distributions across different domains and achieve invariant representations using transfer learning concepts.
- We propose a Transformer-based booster to enhance descriptor robustness by integrating the global descriptors and positional information through the concepts of amplitude and phase of waves.

- We develop a hierarchical feature aggregation network incorporating these two key components with carefully designed loss functions to achieve **R**obust and **A**ccurate feature Learning with **D**omain **A**daptation (RADA).

## 2 Related Works

### 2.1 Local Feature Learning

Descriptors were predominantly hand-crafted initially, with SIFT and ORB [10] being the most representative examples. The advent of deep learning has significantly advanced the performance of learned local descriptors. Most patch-based learning descriptors [22] adopt the network architecture introduced in L2-Net [21], each with different loss functions. However, these methods primarily focus on descriptor extraction, with their receptive fields limited to the image patch. Other descriptors [34], following the 'detect-then-describe' paradigm (score map-based methods), estimate score maps and descriptor maps, where the score map indicates keypoint probability.

ALIKE [34] introduces a differentiable keypoint detection module based on the score map, enabling backpropagation of gradients and subpixel-level keypoint production. Additionally, joint detection and description methods have shown increasing performance. SuperPoint [5] proposes a network trained on homography image pairs. R2D2 [16] computes the repeatability and reliability maps for keypoint detection. DISK [24] employs reinforcement learning to train both score and descriptor map. D2-Net [6] detects keypoints using channel and spatial maxima on low-resolution feature maps. ASLFeat [14] uses multi-level features to detect keypoints and models the local shape with deformable convolutions, enhancing localization accuracy and descriptors.

Despite numerous related works focusing on learning local features, there is limited attention on enhancing descriptor robustness and accuracy through domain adaptation and the implementation techniques of domain supervision.

### 2.2 Domain Adaptation

Domain adaptation aims to bridge the gap between features learned from networks across source and target data. This concept has been extensively developed through deep learning, enhancing adaptation performance in computer vision and multimedia applications [25,29]. Several methods [26] employ the Maximum Mean Discrepancy (MMD) [15] loss, which computes the norm of the difference between two domain means, to minimize the difference of their feature distributions. Other approaches [25] motivate from adversarial learning, with the gradient reversal algorithm (ReverseGrad) from DANN [7] being particularly relevant. This algorithm treats domain invariance as a binary classification problem, directly maximizing the loss of the domain classifier by reversing its gradients to learn a representation that is simultaneously discriminative of source labels while indistinguishable between domains.

In local feature learning tasks, DomainFeat [30] is the first to introduce domain adaptation to the field, developing image-level domain invariance supervision by fusing domain-invariant representations. Motivated by these advancements, we implement our domain adaptation supervision, which organically combines the MMD loss and gradient reversal algorithm to learn accurate and robust features across different domains.

### 2.3 Feature Context Awareness

The distribution of feature locations and descriptors within an entire image forms a global context, and incorporating this into descriptors has become a rising trend in local feature matching methods [19]. ContextDesc [13] encodes both geometric and visual contexts by using keypoint locations, raw local features, and high-level regional features as inputs. MTLDesc [27] introduces an adaptive global context enhancement module and multiple local context enhancement modules to inject non-local contextual information, thereby efficiently learning high-level dependencies between distant features. FeatureBooster [28] only takes the descriptors and geometric information, such as 2D locations, as inputs and uses a lightweight Transformer to aggregate them and produce new descriptors.

However, most of these works use MLPs as position encoders, which have relatively weak encoding abilities. Inspired by Wave-MLP [20,12], we recognize that phase information is equally important as amplitude information in vectors. We encode the descriptor as amplitude information and the position as phase information, then fuse the visual and geometric information using the Euler formula to generate position-aware descriptors in the Transformer-based booster.

## 3 Methodology

### 3.1 Backbone

The procedure of our network to learn global domain-invariant features includes feature encoding, feature aggregation, and local feature extraction. Starting from an input image  $I \in \mathbb{R}^{H \times W \times 3}$ , the process proceeds to generate a score map  $S \in \mathbb{R}^{H \times W}$  and a descriptor map  $D \in \mathbb{R}^{H \times W \times dim}$ , and finally identifies sub-pixel keypoints  $\{p = [u, v]^T\}$  along with their corresponding descriptors  $\{d \in \mathbb{R}^{dim}\}$ .

**Feature Encoding:** The feature encoder transforms the input image  $I$  into multi-scale features  $F_1, F_2, F_3, F_4$  using four encoding blocks with channel ranges of 32, 64, 128, and 128. The first block consists of two-layer  $3 \times 3$  convolutions with ReLU activation that extract low-level image features  $F_1$ . The last three blocks contain a max-pooling layer and a  $3 \times 3$  basic ResNet block. The downsample rate of max-pooling in block 2 is 0.5, and 0.25 in blocks 3 and 4.

**Feature aggregation:** It combines multi-scale features  $F_1, F_2, F_3, F_4$  to enhance both localization and representation capabilities. We use a  $1 \times 1$  convolution and a bilinear upsampling layer for the hierarchical features to align their dimensions and resolutions. By concatenating these aligned features, we obtain the aggregated feature  $F$  for the next keypoint detection and descriptor extraction.

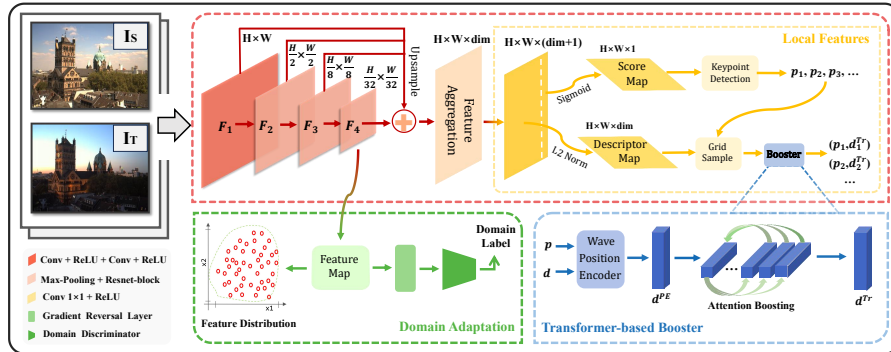


Fig. 2: Network architecture. Our RADA consists of three components: keypoint detection and descriptor extraction backbone to learn accurate descriptors from hierarchical features, domain adaptation supervision to achieve domain-invariant representations, and a Transformer-based booster to enhance the robustness of descriptors. The cross-domain training image pairs with ground truth are produced from Megadepth [9].

**Feature extraction:** This component first produces an  $H \times W \times (dim + 1)$  feature map, which consists of two main components. The first  $dim$  channels are L2 normalized to form the descriptor map  $D$  and the last channel is normalized using Sigmoid activation to create the score map  $S$ . A Differentiable Keypoint Detection (DKD) module [34] is applied to detect trainable, differentiable keypoints. It first uses non-maximum suppression (NMS) on the score map  $S$  to identify local maxima, and then refines the positions of these pixel-level keypoints with softargmax on the local patches, extracting differentiable subpixel keypoints. Based on the accurate keypoints, the network then samples their corresponding descriptors from the dense descriptor map  $D$ . Finally, the keypoints and descriptors are further enhanced through the Transformer-based booster described in section 3.3, resulting in accurate local features.

### 3.2 Domain Adaptation Supervision

For the source domain image  $I_S$  and the transformed target domain image  $I_T$ , the inconsistency between their feature domains can disrupt the processing of keypoint detection and descriptor extraction.

As shown in Fig. 3a, to align the distribution between the high-level feature maps of  $I_S$  and  $I_T$ , we first apply the Maximum Mean Discrepancy (MMD) metric [15] with a linear kernel function. This distance is computed with respect to a particular representation,  $\phi(\cdot)$ , operating on source domain high-level features,  $x_s \in X_S$ , and target domain high-level features,  $x_t \in X_T$ . The empirical

approximation of this distance is computed as follows:

$$\mathcal{L}_{\text{MMD}}(X_S, X_T) = \left\| \frac{1}{|X_S|} \sum_{x_s \in X_S} \phi(x_s) - \frac{1}{|X_T|} \sum_{x_t \in X_T} \phi(x_t) \right\|. \quad (1)$$

Next, we apply a gradient reversal layer [7] to implement domain adversarial learning, making the adversarial discriminator indistinguishable between domains. This is followed by fully connected layers with channels to (dim, 512, 128), culminating in a binary classifier. The domain classifier distinguishes the global domain-invariant features ( $X_S, X_T$ ) with the cross-entropy loss:

$$\mathcal{L}_{\text{adv}}(X_S, X_T) = \frac{1}{N} \sum_{i=1}^N (-l_i \log(s_i) - (1 - l_i) \log(1 - s_i)), \quad (2)$$

where  $l_i$  denotes the domain category label of the image:  $l_i = 1$  for the target image  $I_T$ , and  $l_i = 0$  for the source image  $I_S$ .  $s_i$  represents the domain prediction score of the target image  $I_T$ .

During forward propagation, the features of the gradient reversal layer remain unchanged, whereas during back propagation, the gradient returned by the gradient reversal layer maximizes the loss function, updating the parameters in the direction of the negative gradient. It minimizes the distribution distance and maximizes the domain classifier loss, resulting in domain-invariant features. This process weakens the discrimination between the target and source images for the discriminator network, mapping the feature domains of the two images as closely as possible, thereby improving network performance. Finally, we define the loss function of the domain adaptation supervision as:

$$\mathcal{L}_{\text{da}} = \mathcal{L}_{\text{adv}} + \lambda \mathcal{L}_{\text{MMD}}. \quad (3)$$

### 3.3 Transformer-based Booster

Given  $N$  detected keypoints in the image  $I$ , their positions  $p \in \mathbb{R}^{N \times 3}$  and descriptors  $d \in \mathbb{R}^{N \times C}$  are dynamically fused using a Wave Position Encoder (Wave-PE) to enhance descriptor robustness. The global context, encompassing descriptors of other features and the spatial layout of all features, is then integrated using a Transformer. This incorporation of global information significantly enhances the robustness of individual descriptors, resulting in improved performance under challenging domain variations.

**Wave Position Encoder** strengthens descriptors with more information by fusing position and descriptor information through amplitude and phase relationships. This method offers a stronger encoding capacity compared to traditional MLP-based position encoders.

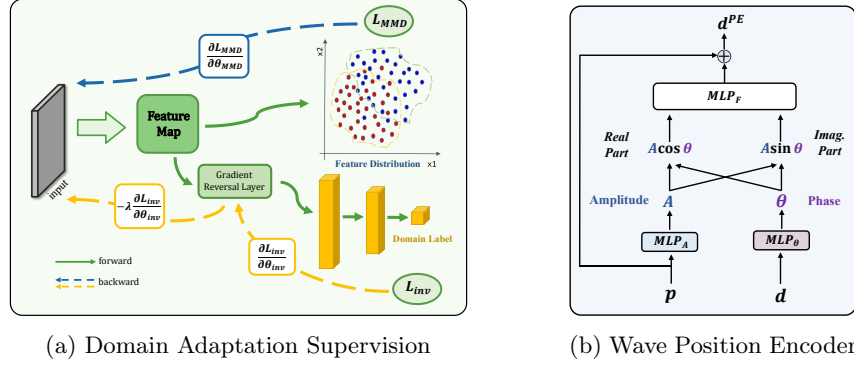


Fig. 3: Clear illustration of the two modules. (a) Domain adaptation is achieved by adding a domain classifier connected to the feature map via a gradient reversal layer. (b) Wave-PE fuses the amplitude  $A$  estimated with the descriptor  $d$  and the phase  $\theta$  estimated with the position  $p$  to generate position encoding.

In Wave-PE, position encoding is represented as a wave  $\tilde{w}$  with both amplitude  $A$  and phase  $\theta$  information. The Euler formula is employed to decompose waves into real and imaginary parts, allowing efficient processing:

$$w_j = A_j \odot e^{i\theta_j} = A_j \odot \cos \theta_j + i \cdot A_j \odot \sin \theta_j, \quad j = 1, 2, \dots, n. \quad (4)$$

As shown in Fig. 3b, the amplitude and phase are estimated by two learnable networks via descriptors and positions, respectively. A learnable network then fuses the real and imaginary parts into position encoding:

$$\begin{aligned} A_j &= \text{MLP}_A(d_j), \quad \theta_j = \text{MLP}_\theta(p_j), \\ d_j^{\text{PE}} &= d_j + \text{MLP}_F([A_j \odot \cos \theta_j, A_j \odot \sin \theta_j]), \end{aligned} \quad (5)$$

where  $[\cdot, \cdot]$  denotes concatenation. For simplicity, a two-layer MLP is used for the networks in eq. (5).

**Attention-Free Transformer** (AFT) offers lower time and space complexity compared to the traditional multi-head attention (MHA) mechanism used in vanilla Transformers. Inspired by FeatureBooster [28], we use AFT-attention [32] to aggregate all local feature information, forming a global context that enhances descriptor robustness. AFT rearranges the computation order of  $Q$ ,  $K$ ,  $V$ , and then multiplies  $K$  and  $V$  element-wise instead of using matrix multiplication. The Attention-Free Transformer for keypoint  $i$  is formulated as:

$$\begin{aligned} f_i(X) &= \sigma(Q_i) \odot \frac{\sum_{j=1}^N \exp(K_j) \odot V_j}{\sum_{j=1}^N \exp(K_j)} \\ &= \sigma(Q_i) \odot \sum_{j=1}^N (\text{softmax}(K) \odot V)_j, \end{aligned} \quad (6)$$

where  $\sigma(\cdot)$  is a Sigmoid function;  $Q_i$  represents  $i$ -th row of  $Q$ , and  $K_j, V_j$  represent the  $j$ -th rows of  $K, V$ . AFT performs a revised version of the MHA operation where the number of attention heads equals the model’s feature dimension  $D$ , and the similarity used in MHA is replaced by a kernel function  $sim(Q, K) = \sigma(Q) \cdot softmax(K)$ . In this way, attention can be computed by element-wise multiplication instead of matrix multiplication, resulting in a time and space complexity that is linear with context and feature size. Thus, the distinguishability of local features can be improved.

Following previous work [16,28], we treat descriptor matching as a nearest neighbor retrieval problem and use Average Precision (AP) to train the descriptors [4]. The attention-boosted local feature descriptors,  $\{d_1^{PE}, d_2^{PE}, \dots, d_N^{PE}\} \rightarrow d_j^{Tr}$ , are optimized to maximize AP for all descriptors  $d^{Tr}$ , with the training goal to minimize the following cost function:

$$\mathcal{L}_{Tr} = 1 - \frac{1}{N} \sum_{i=1}^N AP(d_j^{Tr}). \quad (7)$$

### 3.4 The Loss Functions

In addition to the domain adaptation loss and Transformer-based boosting loss described above, we also define the detector loss, descriptor loss and coupling loss for the entire supervision training. To supervise the features, we adopt the reprojection loss and the neural reprojection error (NRE) loss proposed in [34].

Considering an image pair  $(I_A, I_B)$ , the network extracts score maps  $S_A$  and  $S_B$  from the image pair. The DKD module then detects the keypoints  $P_A \in \mathbb{R}^{N_A \times 2}$  and  $P_B \in \mathbb{R}^{N_B \times 2}$ , respectively. Corresponding descriptors for  $P_A$  and  $P_B$  are denoted by  $D_A \in \mathbb{R}^{N_A \times dim}$  and  $D_B \in \mathbb{R}^{N_B \times dim}$ , respectively. We define the loss functions as follows:

**Detector Loss** is defined as the reprojection loss. Since the keypoints extracted are differentiable, we can directly train their positions using the reprojection distance. For a keypoint  $p_A$  in image  $I_A$ , we warp it to image  $I_B$  using 3D perspective projection:

$$p_{AB} = \mathbf{wrap}_{AB}(p_A) = \pi(d_A R_{AB} \pi^{-1}(p_A) + t_{AB}), \quad (8)$$

where  $R_{AB}$  and  $t_{AB}$  denote the rotation and translation matrices from  $I_A$  to  $I_B$ , respectively.  $d_A$  represents the depth of  $p_A$ , and  $\pi(p)$  is the process of projecting a 3D point  $P = [X, Y, Z]^T$  onto the image plane. In  $I_B$ , we search for the nearest keypoint  $p_B$  to  $p_{AB}$ , ensuring their distance is less than  $th_{gt}$  pixels. This keypoint  $p_B$  is considered the matching keypoint of  $p_A$ . Similarly, we project  $p_B$  back to  $I_A$  to obtain  $p_{BA}$ . The reprojection loss of  $(p_A, p_B)$  is:

$$\mathcal{L}_{det}(p_A, p_B) = \frac{1}{2} (\|p_A - p_{BA}\| + \|p_B - p_{AB}\|). \quad (9)$$

The overall reprojection loss  $\mathcal{L}_{det}$  is then calculated as the average reprojection loss of all matching keypoints in both images.



**Descriptor Loss** abandons the classical triplet loss and adopts the NRE loss [8] to optimize the dense descriptor map. It minimizes the cross-entropy difference between the dense reprojection probability map and the dense matching probability map, thereby providing a comprehensive constraint for the dense descriptor map and a stable training process.

For a keypoint  $p_A$  in image  $I_A$ , and its reprojected keypoint  $p_{AB}$  in image  $I_B$ , the reprojection probability map is defined by  $p_{AB}$  using the bilinear interpolation as in [34]:  $q_r(p_A|p_{AB})$ . For the descriptor  $d_{p_A} \in \mathbb{R}^{dim}$  of keypoint  $p_A$  and the dense descriptor map  $D_B \in \mathbb{R}^{(H \times W) \times dim}$ , their matching probability map is given as the softmax normalization:

$$q_m(p_B | d_{p_A}, D_B) := \text{softmax} \left( \frac{D_B \cdot d_{p_A} - 1}{t_{des}} \right), \quad (10)$$

where  $t_{des}$  controls the sharpness of matching probability map. The NRE loss [8] minimizes the difference between the reprojection probability map and the matching probability map using cross-entropy (CE):

$$\begin{aligned} NRE(p_A, I_B) &:= \text{CE}(q_r(p_B | p_{AB}) \| q_m(p_B | d_{p_A}, D_B)) \\ &= -\ln(q_m(p_{AB} | d_{p_A}, D_B)). \end{aligned} \quad (11)$$

Thus, we define the descriptor loss in a symmetric way as:

$$\mathcal{L}_{des} = \frac{1}{N_A + N_B} \left( \sum_{p_A \in I_A} NRE(p_A, I_B) + \sum_{p_B \in I_B} NRE(p_B, I_A) \right), \quad (12)$$

where  $N_A$  and  $N_B$  are the number of keypoints in image  $I_A$  and  $I_B$ , respectively.

**Coupling Loss** constraints the keypoints in discriminative areas to improve their reliability with the assistance of descriptors. Inspired by methods following the 'detect-and-describe' paradigm like D2-Net [6], we define it as:

$$\mathcal{L}_{cp}^A = \frac{1}{N_A} \sum_{\substack{p_A \in I_A \\ p_{AB} \in I_B}} \frac{s_{p_A} s_{p_{AB}}}{\sum_{\substack{p'_A \in I_A \\ p'_{AB} \in I_B}} s_{p'_A} s_{p'_{AB}}} \mathcal{M}(p_{AB}, d_{p_A}, D_B), \quad (13)$$

where  $N_A$  is the number of keypoints in the image  $I_A$ . For each keypoint  $p_A$  in image  $I_A$ ,  $p_{AB}$  is its corresponding projection keypoint in image  $I_B$ .  $s_p$  denotes the score value of keypoint  $p$  in its corresponding image. Specially, we define the ranking loss  $\mathcal{M}()$  for representation learning as:

$$\mathcal{M}(p_{AB}, d_{p_A}, D_B) = 1 - \mathcal{S} \left( \exp \left( \frac{D_B \cdot d_{p_A} - 1}{t_{des}} \right), p_{AB} \right), \quad (14)$$

where  $\mathcal{S}(\cdot, \cdot)$  is the bilinear sampling at position  $\in \mathbb{R}^2$  and probability map  $\in \mathbb{R}^{H \times W}$ . Similarly, the overall coupling loss is given symmetrically as:

$$\mathcal{L}_{cp} = \frac{1}{2} (\mathcal{L}_{cp}^A + \mathcal{L}_{cp}^B). \quad (15)$$

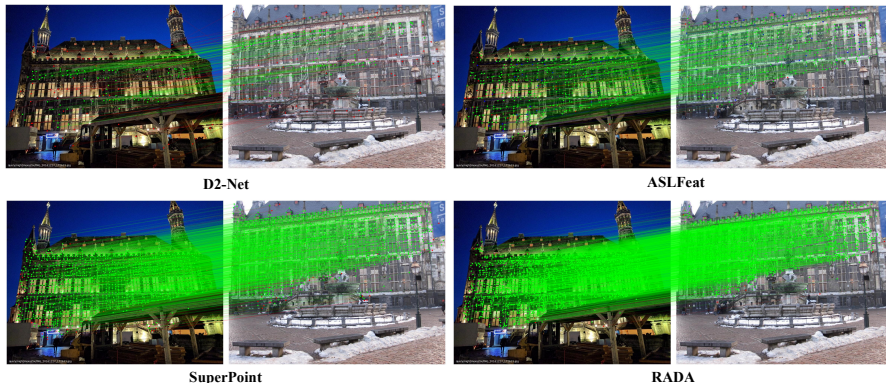


Fig. 4: Visualization of matches on Aachen Day-Night [33]. The inliers are plotted in green if they are correct (0 to 5 pixels in reprojection error), in red if they are incorrect (above 5 pixels), and in blue if ground truth depth is not available.

**Total Loss** combines these loss functions, each with its own coefficient:

$$\mathcal{L}_{\text{total}} = \omega_{\text{da}}\mathcal{L}_{\text{da}} + \omega_{\text{Tr}}\mathcal{L}_{\text{Tr}} + \omega_{\text{det}}\mathcal{L}_{\text{det}} + \omega_{\text{des}}\mathcal{L}_{\text{des}} + \omega_{\text{cp}}\mathcal{L}_{\text{cp}}. \quad (16)$$

## 4 Experiments

### 4.1 Implementation Details

**Training Data:** We trained our RADA on MegaDepth [9] and adopted the training scenes used in DISK [24]. We followed the cross-domain data preparation strategy proposed in [30], using HiDT [2] to translate the source domain images  $I_S$  to dusk and evening image domains  $I_T$ . Since the target domain images also come from MegaDepth, they correspond to images with ground truth correspondence. We then computed the overlap score between two images following D2-Net [6] and sampled 100 training pairs with an overlap score in the range of [0.3, 1] for each scene at every epoch.

**Training Details:** The radius of the differential keypoints detection part is set to 2 pixels, and keypoints with reprojection distances of less than 5 pixels are considered ground truth keypoint pairs during training. The coefficients of the overall loss eq. (16),  $(\omega_{\text{da}}, \omega_{\text{Tr}}, \omega_{\text{det}}, \omega_{\text{des}}, \omega_{\text{cp}})$  are optimized by Optuna [1] as  $(2, 1, 1, 5, 1)$ , and  $\lambda$  in eq. (3) is set as 0.01. The images were cropped and resized to  $480 \times 480$  during training. The network was trained using the ADAM optimizer, with the learning rate starting at zero and warming up to  $3e^{-3}$  over 500 steps before remaining constant. We set the batch size to 2 and accumulated gradients over 16 batches. Under these settings, the proposed model converges on a single NVIDIA RTX 4090 in about 30 hours.

Table 1: GFLOPs and FPS on  $640 \times 480$  images, illumination and overall MMA within one to three pixels thresholds of different methods on HPatches [3]. The top three results are marked with **red**, **green**, **blue**. \* represents similar results.

Models	GFLOPs	FPS	MMA <sub>i@1</sub>	MMA <sub>i@2</sub>	MMA <sub>i@3</sub>	MMA@1	MMA@2	MMA@3
D2-Net [6]	889.40	6.60	13.76%	29.01%	43.22%	9.78%	23.52%	37.29%
SuperPoint [5]	<b>26.11</b>	<b>45.87</b>	43.09%	59.39%	69.25%	34.27%	54.94%	66.37%
R2D2 [16]	464.55	8.70	37.60%	66.08%	<b>80.78%</b>	33.31%	62.17%	<b>75.77%</b>
ASLFeat [14]	<b>44.24</b>	8.96	46.12%	64.46%	75.45%	39.16%	61.07%	72.44%
DISK [24]	98.97	15.73	<b>51.98%</b>	<b>77.11%</b>	<b>82.61%</b>	<b>43.71%</b>	<b>66.98%</b>	<b>77.59%</b>
ALIKE [34]	<b>67.63*</b>	<b>29.15</b>	<b>51.24%</b>	<b>69.51%</b>	77.40%	<b>44.97%</b>	<b>66.21%</b>	74.51%
RADA	<b>67.74*</b>	<b>24.56</b>	<b>52.13%</b>	<b>70.83%</b>	<b>78.65%</b>	<b>45.03%</b>	<b>67.17%</b>	<b>76.24%</b>

## 4.2 Image Matching

**Experiment setup:** HPatches [3] is a common evaluation dataset for image matching, including 116 scenes and 580 image pairs, which exhibit significant changes in illumination or viewpoints. This dataset provides ground truth homography between each image pair for evaluation. Following the protocol of D2-Net, we exclude 8 high-resolution sequences from the 116 available sequences and use 108 sequence scenes with viewpoint or illumination changes for a fair comparison. We record the mean matching accuracy (MMA), the average percentage of correct matches to all estimated putative matches, under thresholds varying from one to ten pixels, along with the numbers of features and matches. Specially, We evaluate the MMA@3 without loss of generality. We also record GFLOPs (Giga Floating-point Operations) and the interface FPS (Frames Per Second), which represent the computing complexity and response speed. Like D2-Net, we use mutual nearest neighbor search as the matching method.

**Results:** Table 1 shows the results on HPatches under illumination and overall change. Our method generally outperforms other proposed methods. Although R2D2 [16] and DISK [24] sometimes perform better on different evaluation metrics, they sacrifice either the computing complexity or the response speed. Our RADA balances accuracy, computing complexity, and response speed organically, resulting in better overall performance.

Table 2: Ablation studies of network architecture and losses. *DET*, *DES*, and *CP* denote detector loss, descriptor loss and coupling loss, respectively.

Methods	MMA@3	DET	DES	CP	MMA@3
<b>Backbone</b>	70.48%		✓	✓	71.86%
+ Domain Adaptation Supervision	74.72%	✓	✓		68.92%
+ Transformer-based Booster	<b>76.24%</b>	✓	✓	✓	<b>76.24%</b>

**Ablation:** We conduct ablation studies on HPatches to explore the performance of our two special components and architecture loss functions. We evaluate the MMA@3 without loss of generality as shown in Table 2. The domain adaptation supervision ensures the network learns domain-invariant features, and the Transformer-based booster enhances the accuracy and robustness of features, consistent with the ablation study outcomes. The detector loss directly optimizes keypoints positions to produce accurate keypoints, while the coupling loss ensures that the keypoints are located in areas where the descriptors are discriminative. More reliable keypoints produce fewer false matches, resulting in a higher matching accuracy.

### 4.3 Visual Localization

**Experiment setup:** We evaluate our method in visual localization, a more complete pipeline in computer vision. We select an outdoor dataset with severe illumination changes, Aachen Day-Night dataset v1.1[33], which contains 6697 day-time database images and 1015 query images (824 for the day and 191 for the night). We use the hierarchical localization toolbox (HLoc)[18] by replacing the feature extraction module with different feature detectors and descriptors. We use the evaluation protocol on the Long-Term Visual Localization Benchmark[23] and report the percentage of correct localized query images under given error thresholds. Note that all other methods use mutual nearest neighbor search for matching. We utilize ratio test or distance test for mutual nearest neighbor matching, whose thresholds are same as setting in [28].

**Results:** The results are shown in Table 3. This demonstrates that our descriptor based on domain adaptation has significantly improved the performance of the descriptor and is efficiently combined with keypoints detection under the day-night domain changes. As shown in Fig. 4, our method can detect more accurate keypoints and generate effective matches under the same conditions, and the descriptors of keypoint locations have higher discriminability. Thus, learn-

Table 3: Visual localization results in Aachen Day-Night [33]. The positional and angular performances are present (the larger the better). The top two results are marked with red, green.

Method	Day	Night
	$(0.25m, 2^\circ) / (0.50m, 5^\circ) / (5.0m, 10^\circ)$	
SIFT[10]	87.1 / 93.8 / 98.1	50.8 / 70.2 / 81.2
SuperPoint[5]	87.9 / 94.3 / 98.2	67.0 / 84.8 / 95.8
SOSNet[22]	<u>88.7</u> / <u>94.7</u> / 98.7	58.1 / 78.5 / 92.7
R2D2[16]	86.8 / 94.1 / 98.4	57.1 / 76.4 / 88.5
DISK[24]	86.9 / 93.3 / <u>99.2</u>	<u>69.4</u> / <u>86.8</u> / 96.7
ALIKE[34]	87.3 / 93.2 / 98.7	67.5 / 85.3 / <u>97.9</u>
RADA	<u>87.9</u> / <u>94.4</u> / <u>99.0</u>	<u>72.9</u> / <u>86.8</u> / <u>98.6</u>

ing descriptors with domain adaptation can effectively increase the accuracy of challenging visual localization tasks.

## 5 Conclusion

In this study, we develop RADA, a multi-level feature aggregation network incorporating domain adaptation supervision and Transformer-based booster, to learn robust and accurate features under extreme domain shifts. The hierarchical network efficiently captures diverse features to achieve accurate keypoint detection and descriptor extraction. By aligning the high-level feature distributions across different domains, the domain adaptation supervision ensures the learning of invariant domain representations. The Transformer-based booster integrating visual and geometric information is proposed to enhance the robustness of descriptors. To ensure the accuracy and robustness of features, we propose three additional losses to apply targeted supervision on keypoint detection, descriptor extraction, and their coupled processing. Comprehensive experiments conducted in image matching and visual localization tasks validate the superiority of our method in these applications.

## References

1. Akiba, T., Sano, S., Yanase, T., Ohta, T., Koyama, M.: Optuna: A next-generation hyperparameter optimization framework. In: Proceedings of the 25th ACM SIGKDD international conference on knowledge discovery & data mining. pp. 2623–2631 (2019)
2. Anokhin, I., Solovev, P., Korzhenkov, D., Kharlamov, A., Khakhulin, T., Silvestrov, A., Nikolenko, S., Lempitsky, V., Sterkin, G.: High-resolution daytime translation without domain labels. In: Proceedings of the IEEE/CVF Conference on Computer Vision and Pattern Recognition. pp. 7488–7497 (2020)
3. Balntas, V., Lenc, K., Vedaldi, A., Mikolajczyk, K.: Hpatches: A benchmark and evaluation of handcrafted and learned local descriptors. In: Proceedings of the IEEE conference on computer vision and pattern recognition. pp. 5173–5182 (2017)
4. Boyd, K., Eng, K.H., Page, C.D.: Area under the precision-recall curve: point estimates and confidence intervals. In: Machine Learning and Knowledge Discovery in Databases: European Conference, ECML PKDD 2013, Prague, Czech Republic, September 23-27, 2013, Proceedings, Part III 13. pp. 451–466. Springer (2013)
5. DeTone, D., Malisiewicz, T., Rabinovich, A.: Superpoint: Self-supervised interest point detection and description. In: Proceedings of the IEEE conference on computer vision and pattern recognition workshops. pp. 224–236 (2018)
6. Dusmanu, M., Rocco, I., Pajdla, T., Pollefeys, M., Sivic, J., Torii, A., Sattler, T.: D2-net: A trainable cnn for joint detection and description of local features. arXiv preprint arXiv:1905.03561 (2019)
7. Ganin, Y., Lempitsky, V.: Unsupervised domain adaptation by backpropagation. In: International conference on machine learning. pp. 1180–1189. PMLR (2015)
8. Germain, H., Lepetit, V., Bourmaud, G.: Neural reprojection error: Merging feature learning and camera pose estimation. In: Proceedings of the IEEE/CVF Conference on Computer Vision and Pattern Recognition. pp. 414–423 (2021)

9. Li, Z., Snavely, N.: Megadepth: Learning single-view depth prediction from internet photos. In: Proceedings of the IEEE conference on computer vision and pattern recognition. pp. 2041–2050 (2018)
10. Lowe, D.G.: Distinctive image features from scale-invariant keypoints. *International journal of computer vision* **60**, 91–110 (2004)
11. Lu, X., Du, S.: Raising the ceiling: Conflict-free local feature matching with dynamic view switching. In: Proceedings of the European Conference on Computer Vision (ECCV) (2024)
12. Lu, X., Yan, Y., Kang, B., Du, S.: Paraformer: Parallel attention transformer for efficient feature matching. In: Proceedings of the AAAI Conference on Artificial Intelligence. vol. 37, pp. 1853–1860 (2023)
13. Luo, Z., Shen, T., Zhou, L., Zhang, J., Yao, Y., Li, S., Fang, T., Quan, L.: Contextdesc: Local descriptor augmentation with cross-modality context. In: Proceedings of the IEEE/CVF conference on computer vision and pattern recognition. pp. 2527–2536 (2019)
14. Luo, Z., Zhou, L., Bai, X., Chen, H., Zhang, J., Yao, Y., Li, S., Fang, T., Quan, L.: Aslfeat: Learning local features of accurate shape and localization. In: Proceedings of the IEEE/CVF conference on computer vision and pattern recognition. pp. 6589–6598 (2020)
15. Quiñero-Candela, J., Sugiyama, M., Schwaighofer, A., Lawrence, N.: Covariate shift and local learning by distribution matching. *Dataset Shift in Machine Learning* pp. 131–160 (2008)
16. Revaud, J., De Souza, C., Humenberger, M., Weinzaepfel, P.: R2d2: Reliable and repeatable detector and descriptor. *Advances in neural information processing systems* **32** (2019)
17. Rublee, E., Rabaud, V., Konolige, K., Bradski, G.: Orb: An efficient alternative to sift or surf. In: 2011 International conference on computer vision. pp. 2564–2571. Ieee (2011)
18. Sarlin, P.E., Cadena, C., Siegwart, R., Dymczyk, M.: From coarse to fine: Robust hierarchical localization at large scale. In: CVPR (2019)
19. Sarlin, P.E., DeTone, D., Malisiewicz, T., Rabinovich, A.: Superglue: Learning feature matching with graph neural networks. In: Proceedings of the IEEE/CVF conference on computer vision and pattern recognition. pp. 4938–4947 (2020)
20. Tang, Y., Han, K., Guo, J., Xu, C., Li, Y., Xu, C., Wang, Y.: An image patch is a wave: Phase-aware vision mlp. In: Proceedings of the IEEE/CVF conference on computer vision and pattern recognition. pp. 10935–10944 (2022)
21. Tian, Y., Fan, B., Wu, F.: L2-net: Deep learning of discriminative patch descriptor in euclidean space. In: Proceedings of the IEEE Conference on Computer Vision and Pattern Recognition (CVPR) (July 2017)
22. Tian, Y., Yu, X., Fan, B., Wu, F., Heijnen, H., Balntas, V.: Sosnet: Second order similarity regularization for local descriptor learning. In: Proceedings of the IEEE/CVF conference on computer vision and pattern recognition. pp. 11016–11025 (2019)
23. Toft, C., Maddern, W., Torii, A., Hammarstrand, L., Stenborg, E., Safari, D., Okutomi, M., Pollefeys, M., Sivic, J., Pajdla, T., et al.: Long-term visual localization revisited. *IEEE Transactions on Pattern Analysis and Machine Intelligence* **44**(4), 2074–2088 (2020)
24. Tyszkiewicz, M., Fua, P., Trulls, E.: Disk: Learning local features with policy gradient. *Advances in Neural Information Processing Systems* **33**, 14254–14265 (2020)

25. Tzeng, E., Hoffman, J., Saenko, K., Darrell, T.: Adversarial discriminative domain adaptation. In: Proceedings of the IEEE conference on computer vision and pattern recognition. pp. 7167–7176 (2017)
26. Tzeng, E., Hoffman, J., Zhang, N., Saenko, K., Darrell, T.: Deep domain confusion: Maximizing for domain invariance. arXiv preprint arXiv:1412.3474 (2014)
27. Wang, C., Xu, R., Zhang, Y., Xu, S., Meng, W., Fan, B., Zhang, X.: Mtl Desc: Looking wider to describe better. In: Proceedings of the AAAI Conference on Artificial Intelligence. vol. 36, pp. 2388–2396 (2022)
28. Wang, X., Liu, Z., Hu, Y., Xi, W., Yu, W., Zou, D.: Featurebooster: Boosting feature descriptors with a lightweight neural network. In: Proceedings of the IEEE/CVF Conference on Computer Vision and Pattern Recognition. pp. 7630–7639 (2023)
29. Xia, H., Zhao, H., Ding, Z.: Adaptive adversarial network for source-free domain adaptation. In: Proceedings of the IEEE/CVF international conference on computer vision. pp. 9010–9019 (2021)
30. Xu, R., Wang, C., Xu, S., Meng, W., Zhang, Y., Fan, B., Zhang, X.: Domainfeat: Learning local features with domain adaptation. IEEE Transactions on Circuits and Systems for Video Technology **34**(1), 46–59 (2023)
31. Xu, S., Chen, S., Xu, R., Wang, C., Lu, P., Guo, L.: Local feature matching using deep learning: A survey. Information Fusion **107**, 102344 (2024)
32. Zhai, S., Talbott, W., Srivastava, N., Huang, C., Goh, H., Zhang, R., Susskind, J.: An attention free transformer. arXiv preprint arXiv:2105.14103 (2021)
33. Zhang, Z., Sattler, T., Scaramuzza, D.: Reference pose generation for long-term visual localization via learned features and view synthesis. International Journal of Computer Vision **129**(4), 821–844 (2021)
34. Zhao, X., Wu, X., Miao, J., Chen, W., Chen, P.C., Li, Z.: Alike: Accurate and lightweight keypoint detection and descriptor extraction. IEEE Transactions on Multimedia **25**, 3101–3112 (2022)